Jordanian Journal of Computers and Information Technology (JJCIT), Vol. 10, No. 02, June 2024.

ILLUMINATION ENHANCEMENT OF NIGHTTIME IMAGES USING A REGULATED SINGLE SCALE RETINEX ALGORITHM

Ola A. Basheer[1] and Zohair Al-Ameen[2]

(Received: 14-Jan.-2024, Revised: 11-Mar.-2024, Accepted: 13-Mar.-2024)

ABSTRACT

Nowadays, people are active during the nighttime and take many photos to record their activities. Due to the low-light nature of the environment at nighttime, captured images tend to appear with dimmed and imbalanced illumination, limited contrast, covert noise and diminished colors. Thus, this paper presents a practical algorithm to improve the illumination of nighttime images based on the single-scale retinex model, image processing methods and certain statistical functions. The developed algorithm initiates by converting the image from the RGB into the HSV model. Then, it enhances only the value (V) channel while preserving the H and S channels. Next, estimating the illumination version of the image and calculating the logarithms of both the illumination and original image are performed. Afterward, a logarithmic subtraction occurs and a modified cumulative distribution function of Gumble probability is applied and the result is further enhanced using a logarithmic transform method. These operations produce the processed V channel and a conversion to the RGB format occurs to generate the final output. The proposed algorithm is experimented with by using two datasets, compared to ten different contemporary algorithms and outcomes are evaluated via three sophisticated metrics. Based on the attained results, promising performances by the developed algorithm have been recorded, surpassing the performance of many existing algorithms in various objective, subjective and runtime terms.

KEYWORDS

Nighttime, Image enhancement, Single-scale retinex, Statistical methods.

1. INTRODUCTION

Nighttime is the period from dusk to dawn [37]. Images taken at nighttime are of defective quality and characterized by unbalanced illumination, unpleasant colors, limited contrast and undesirable noise [1]. Due to the significant increase in nighttime photography to visualize large-scale events, such as personal activities, surveillance and speed cams, there has been an urgent need for efficient nighttime image-enhancement algorithms. Thus, this topic has attracted widespread attention by various beneficiaries. Since hardware is constantly improving, most modern devices and computer-vision applications are required to deliver high-quality images [2]. Image enhancement (IE) refers to the operations applied to an image to improve its perceived quality and make it more visually pleasing to the recipient. The primary goal of IE is to change the characteristics of an image to enhance its suitability for a particular activity and viewer without introducing errors [3]. IE techniques must seek to consider two crucial factors: 1) There may be hidden noise in dark areas of nighttime images, so it must be ensured that the noise is suppressed or kept from being amplified when improving the illumination [4]. 2) Preserving the brightness in the already bright areas from being amplified to avoid the state of over-enhancement [5].

Different algorithms have been introduced to help improve the quality of digital images. One concept of interest is the Retinex theory, which is commonly used for image enhancement and owns many versions, such as the single-scale retinex (SSR), multi-scale retinex (MSR) and multi-scale retinex with color restoration (MSRCR) [6]. This research introduces a well-developed SSR algorithm using statistical and image-processing methods for nighttime-image enhancement. The performance of the proposed algorithm has been tested on two datasets, compared to ten contemporary algorithms explained in the related-work section, in addition to evaluating and discussing the results thoroughly. The paper is organized as follows: the 2nd section explains a literature review of recent years' research work, the 3rd section explains the developed algorithm in depth, the 4th section presents the attained results and the 5th section gives a brief conclusion.

1. O. A. Basheer is with the Department of Computer Science, College of Computer Science and Mathematics, University of Mosul, Mosul, Nineveh, Iraq. Email: olaalh9@gmail.com
2. Z. Al-Ameen is with the ICT Research Unit, Computer Center, University of Mosul Presidency, University of Mosul, Mosul, Nineveh, Iraq. Email: qizohair@uomosul.edu.iq

2. RELATED WORK

In recent years, numerous studies have been introduced on improving nighttime images due to their high importance in different real-world applications. The selected studies are reviewed in a newer to older style. In 2024, a method that utilizes gamma correction and merged color spaces is introduced [35], in that the algorithm starts by determining a transmission map (TM) that includes the saturation information of the degraded image in two different color spaces. Next, the calculated TM is transformed into a function that contains the max and mean values and these values are approximated from a poor illumination image by utilizing a gamma-correction approach. After that, an adaptive value-determination algorithm is applied to enhance the image, prevent the over-enhancement phenomenon and generate the output. In 2023, a Gaussian-based model (GM) was developed [34] and this algorithm starts by creating the GM to get the estimated reflectance and illumination information based on the retinex theory. Then, based on the retinex theory, a decomposition in the GM-based operation is applied to the illumination layer and a gradient descent-based approach is implemented to enhance the image's illumination. Lastly, a denoising process based on the total-variation concept is executed on the reflectance layer to reduce the noise and generate the output.

In 2023, a triangle similarity-based algorithm (TS) was presented [33], in that it begins by transforming the image into the HSI color domain and maintaining the hue channel while processing the saturation and intensity channels. Next, a translation-based operation is applied to the saturation channel to improve the color representation. After that, various scaling operations are implemented in the intensity channel to improve the illumination and visual information. Lastly, a transformation to the RGB domain is applied to create the output. In 2022, a structure preservation-based variation model (SPV) was provided [32] and it started by utilizing a variation-coefficient-based concept to improve the illumination information. Next, a total-variation concept is implemented to reduce the noise information in the image. Lastly, these two images are mixed using the retinex concept in an iterative way to generate the output. In 2021, a progressive-recursive network-based algorithm was established [36], in that the method begins by getting the degraded image and sending it to a dual-attention approach to extract the global features. After that, a mixture of residual blocks and recurrent layers is utilized to extract the local features. Based on the extracted local and global features, several recursive operations are applied to enhance the image and create the output.

In 2020, a semi-decoupled decomposition (SDD) algorithm was proposed [7], in that it decomposes the image using the retinex model into reflectance and illumination components in a semi-decoupled manner. The illumination layer is enhanced progressively and the reflectance layer is improved jointly using a specialized total-variation concept. These components are united to create the output. In 2020, a retinex-based multi-phase (RBMP) algorithm was proposed [8], which is initiated by computing the illumination image in a manner akin to the standard SSR algorithm, subtracts the log of the illumination image from the log of the original image using a modified method and then processes the output through a gamma-corrected sigmoid and normalization approaches to generate the output. In 2019, an adaptive image-enhancement (AIE) algorithm was presented [9], where it first transforms the image to the HSV domain and the V channel is processed to isolate the illumination component of the scene through a multi-scale Gaussian function. Afterward, a correction function is implemented *via* the Weber-Fechner law and two outputs are generated by adaptively adjusting the parameters according to the distribution profiles of the illumination components. The output is created by combining both images using a specially-developed approach. Similarly, in 2019, an algorithm named LECARM was developed [10], which began by utilizing illumination-estimating algorithms to calculate the exposure ratio for every pixel. After that, the chosen camera-response model is employed to modify each pixel to achieve the required exposure based on the estimated exposure-ratio map. Lastly, the output is obtained using a specific mapping method.

Moreover, in 2018, a robust retinex model (RRM) algorithm was presented [11], which starts by applying advanced regularization terms for illumination and reflectance approximation. More precisely, it employs one norm to limit the smoothness of the illumination in different regions, joining a fidelity term to highlight the structural details in low-light areas with the gradients of the reflectance to estimate the noise map using a robust Retinex concept. Next, the enhancement is applied using a Lagrange multiplier-based approach to build the output image. In 2016, a fusion-based enhancement (FBE) algorithm was developed [12], which utilizes an illumination-estimation algorithm based on

morphological closure to separate an observed image into reflectance and illumination components. This algorithm generates two images from the illumination image, one with brightness enhancement and the other with contrast enhancement, by applying sigmoid transform and adaptive-histogram equalization. Moreover, two weights are created using a multi-scale process. Lastly, the two images are fused using the determined weights to create the output. In 2016, an algorithm called LIME was proposed [13], which starts by determining the max values of the RGB image, followed by the determination of reflectance and illumination information *via* the retinex model. The illumination information is enhanced using a structure-processing concept, followed by implementing different maps to further boost illumination. The output image is generated by joining the improved-illumination and reflectance components.

As seen from the studied algorithms, different notions were used and the computational cost of each algorithm varies. Most of the proposed algorithms in this field did not reach the required level of enhancement. Thus, the chance remains to develop a new method that can improve the illumination of nighttime images more efficiently. The proposed algorithm differs from existing algorithms in several aspects. First, low computational developments are utilized to make the proposed algorithm efficient and particularly fast in filtering different nighttime images. Second, the utilized developments improve the illumination in a direct and non-iterative way while considering minimal noise augmentation, which is needed as many existing algorithms utilize the iterative feature and their utilized processing steps may amplify the noise, which leads to the requirement of another major step for image denoising, making such algorithms slow and require high computational cost.

3. PROPOSED ALGORITHM

Land and McCann initially proposed the retinex theory [30]. The term "retinex" is derived from the combination of the root terms "retina" and "cortex," which are both essential components of human vision. Retinex is more visually consistent with human vision. This is predicated on the notion that the reflectance and illumination components' collective influence creates the image, as shown in Figure 1.

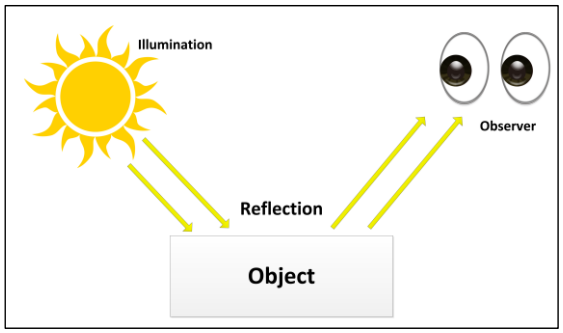

Figure 1. The retinex theory.

Specifically, when light illuminates an object, it creates a reflection that is then seen as an image by the human eye [6]. Various algorithms have been designed based on the retinex theory, such as the SSR [14] and the MSR [15]. Both algorithms utilize a specific Gaussian function to modify a given image. Therefore, the brightness level of the output image is determined by using the natural logarithm of reflectance. Nevertheless, it may exhibit a color-distortion effect, which poses a difficulty in both the SSR and MSR. A potential solution to address this problem is the implementation of a "Multi-scale Retinex with Color Restoration" (MSRCR) technique [16]. Here, the inclusion of MSRCR allows for the handling of color distortion and restoration by utilizing the color ratio of the red, green and blue (RGB) channels. However, due to the universally-applied mapping curve, this method tends to diminish the level of detail in the image, particularly in the areas of high brightness.

The primary motivation of the proposed regulated SSR (RSSR) algorithm is to improve the quality of night images by improving lighting in dark areas without intensifying brighter regions using non-complex concepts. The SSR model and other less-complex statistical concepts and methods were used among these concepts. The original SSR model is used for illumination estimation of degraded images by applying convolution (*) between the input image $I_{(x,y)}$ and the Gaussian function $G_{(x,y)}$, which is calculated in the following manner [17]:

$$G_{(x,y)} = Q \cdot \exp\left(-\frac{\left(U^2 + V^2\right)}{2\sigma^2} \right) \tag{1}$$

$$Q = \frac{1}{\sum_{x=1}^{N}\sum_{y=1}^{M} \exp\left(-\frac{\left(U^2 + V^2\right)}{2\sigma^2} \right)} \tag{2}$$

Let Q be a normalizing factor; x and y represent the coordinates of the digital image; U and V denote two grayscale gradients, where U is horizontal and V is vertical. U and V hold the same size as $I_{(x,y)}$. Additionally, M and N represent the dimensions of $I_{(x,y)}$, $(\cdot)$ denotes a multiplication operation and σ is a parameter that addresses the brightness. Then, the logarithm of the illumination image resulting from the previous step and the logarithm of the degraded image are taken to produce an enhanced version of the degraded image called reflectance image $R_{(x,y)}$ by subtracting the log of the illumination image from the log of the degraded image [14], in the following manner:

$$R_{(x,y)} = \log\left(I_{(x,y)}\right) - \log\left(G_{(x,y)} * I_{(x,y)}\right) \tag{3}$$

where $R_{(x,y)}$ is the output of original SSR. Experiments have been conducted on applying the standard SSR on different nighttime images to determine its filtering abilities with this type of image. Some results are demonstrated in Figure 2.

Figure 2. Outputs of the standard SSR model when applied to different nighttime images.

From the conducted experiments, the SSR provided resulting images with defects, including extra dimming for the darkened areas, which led to the loss of visual details, as well as amplification of brightness in the bright areas and the production of unrealistic colors, leading to overall unacceptable results. Regardless of these defects, the standard SSR model is characterized by low computational cost, which is a key aspect and has a high development potential [14].

The proposed RSSR algorithm aims to improve illumination while producing appropriate colors and avoids the over-amplification of the latent noise. The RSSR algorithm begins its first phase by converting the image from the RGB form into the HSV color model [18]. This color model is designed to efficiently separate the color information from the brightness (value) information, making it intuitive to improve brightness by simply modifying the value component. Supposing that the input image $I_{(x,y)}$ has three color channels of red (R), green (G) and blue (B) and R, G, B $\in$ [0, W_m], with W_m being the max. range value (typically 1), assuming the range $\in$ [0,1], the conversion to the HSV color domain can be achieved using the following equations [31]:

$$S = \frac{W_r}{W_h} \quad \text{for } W_h > 0, \quad 0 \text{ otherwise} \tag{4}$$

$$V = \frac{W_h}{W_m} \tag{5}$$

with W_h, W_l and W_r defined as $W_h = \max(R, G, B)$, $W_l = \min(R, G, B)$, $W_r = (W_h - W_l)$, where S is the saturation channel and V is the value channel. What is more needed is to determine the hue (H) channel, wherein if the three RGB channels contain a similar value, then it is the case of a gray pixel. In this situation, $W_r = 0$, $S = 0$ and H is undefined. To calculate H when $W_r > 0$, each channel is normalized in the following manner:

$$\hat{R} = \frac{W_h - R}{W_r}, \qquad \hat{G} = \frac{W_h - G}{W_r}, \qquad \hat{B} = \frac{W_h - B}{W_r}. \tag{6}$$

Next, the initial hue (Ĥ) is calculated based on the notion of which color channel contains the max. value in the following manner:

$$\hat{H} = \begin{cases} \hat{B} - \hat{G} & \text{if } R = W_h \\ \hat{R} - \hat{B} + 2 & \text{if } G = W_h \\ \hat{G} - \hat{R} + 4 & \text{if } B = W_h \end{cases} \tag{7}$$

The outcome value of Ĥ is in the range of [-1, 5] and the final H channel is obtained in the range of [0,1] as follows:

$$H = \frac{1}{6} \cdot \begin{cases} \left(\hat{H} + 6\right) & \text{for } \hat{H} < 0 \\ \hat{H} & \text{otherwise.} \end{cases} \tag{8}$$

The operations are performed only on the value channel, because the key requirement here is to improve the illumination, as the HSV color domain separates the color information from the illumination information. Thus, the processing becomes rapid and efficient. In the second phase, the Gaussian function $G_{(x,y)}$ is calculated using Eq. (1) and Eq. (2), where ($\sigma = N \times M$). The third phase includes the computation of the illumination image in the following manner [17]:

$$M_{(x,y)} = G_{(x,y)} * I_{(x,y)} \tag{9}$$

where, $M_{(x,y)}$ is the illumination image. To apply the convolution (*) in the frequency domain, first, the Fourier transform is used to convert the inputs from the spatial domain into the frequency domain. Then, the element-wise multiplication between two inputs of the same size is computed. It often needs a frequency shift to return the high frequencies in the middle and the low frequencies in the edges and finally convert the image from the frequency domain into the spatial domain [19]. In the fourth phase, the log of the illumination image $M_{(x,y)}$ and the log of the input image $I_{(x,y)}$ are determined as follows:

$$O_{(x,y)} = \log\left(I_{(x,y)} + \varepsilon\right) \tag{10}$$

$$L_{(x,y)} = \log\left(M_{(x,y)} + \varepsilon\right) \tag{11}$$

Here, ($\varepsilon = 0.001$) represents a minor value added to prevent the computation of the log of zero, which is infinite. The fifth utilized phase includes the application of a logarithmic-subtraction approach [20], as logarithmic image processing has been utilized in dynamic range manipulation, improving the visibility of details in both dark and bright regions, replacing the standard-subtraction method in Eq. (3) to produce the reflectance image, as follows:

$$Z_{(x,y)} = \frac{O_{(x,y)} - L_{(x,y)}}{1 - O_{(x,y)} \cdot L_{(x,y)}} \tag{12}$$

After that, the sixth phase is implemented, which includes the utilization of a slightly modified cumulative distribution function of the Gumble probability (CDF-GP) approach. The standard CDF-GP approach can be mathematically expressed as follows [21]:

$$F_{(x,y)} = \exp\left(-\exp\left(-\frac{(x-\mu)}{\beta}\right)\right) \tag{13}$$

This approach redistributes the values across the image, emphasizing certain brightness levels over others and improves the contrast depending on β. With a slight heuristic modification to simplify the calculation, its equation becomes as follows:

$$F_{(x,y)} = \exp\left(-\exp\left(-\frac{Z_{(x,y)}}{\beta}\right)\right) \tag{14}$$

where $\beta > 0$ is the parameter that controls the image illumination and contrast, in that lower β values compress the range of values, reducing illumination and contrast. In comparison, higher β values spread

out the intensity values, potentially enhancing illumination and contrast. Next, the log transform is applied as the seventh phase to further improve fine details in low-density areas. This transformation is appropriate for an excessively dark image, as it increases the values of dark pixels and decreases the values of highly-illuminated pixels [22], resulting in a well-balanced, visually pleasing outcome. The log transform can be computed as follows [23]:

$$S_{(x,y)} = c \cdot \log\left(F_{(x,y)} + 1\right) \tag{15}$$

where $S_{(x,y)}$ represents the resulting value channel and c is a luminance parameter that is set to 2.5. In the final eighth phase, a conversion from HSV to RGB is applied. To convert the HSV image, where $\in$ [0, 1], to the corresponding RGB image, the following is applied [31]:

$$\hat{H} = (6 \cdot H) \bmod 6 \tag{16}$$

where $(0 \leq \hat{H} < 6)$ is initially obtained, then the intermediate values are calculated as follows:

$$\begin{aligned} c_1 &= \lfloor \hat{H} \rfloor & x &= (1 - S) \cdot v \\ c_2 &= \hat{H} - c_1 & y &= \left(1 - \left(S \cdot c_2\right)\right) \cdot V \\ v &= V & z &= \left(1 - \left(S \cdot (1 - c_2)\right)\right) \cdot V \end{aligned} \tag{17}$$

Using these pre-determined values, the normalized RGB channels are computed as follows:

$$\left(\hat{R}, \hat{G}, \hat{B}\right) = \begin{cases} (v, z, x) & \text{if } c_1 = 0 \\ (y, v, x) & \text{if } c_1 = 1 \\ (x, v, z) & \text{if } c_1 = 2 \\ (x, y, v) & \text{if } c_1 = 3 \\ (z, x, v) & \text{if } c_1 = 4 \\ (v, x, y) & \text{if } c_1 = 5 \end{cases} \tag{18}$$

Finally, scaling the channels to the range of [0, A-1] (normally A = 256) is done in the following manner:

$$\begin{aligned} R &= \min\left(\text{round}\left(A \cdot \hat{R}\right), A - 1\right) \\ G &= \min\left(\text{round}\left(A \cdot \hat{G}\right), A - 1\right) \\ B &= \min\left(\text{round}\left(A \cdot \hat{B}\right), A - 1\right) \end{aligned} \tag{19}$$

where RGB is the final algorithm output. The flowchart of the proposed RSSR algorithm is demonstrated in Figure 3.

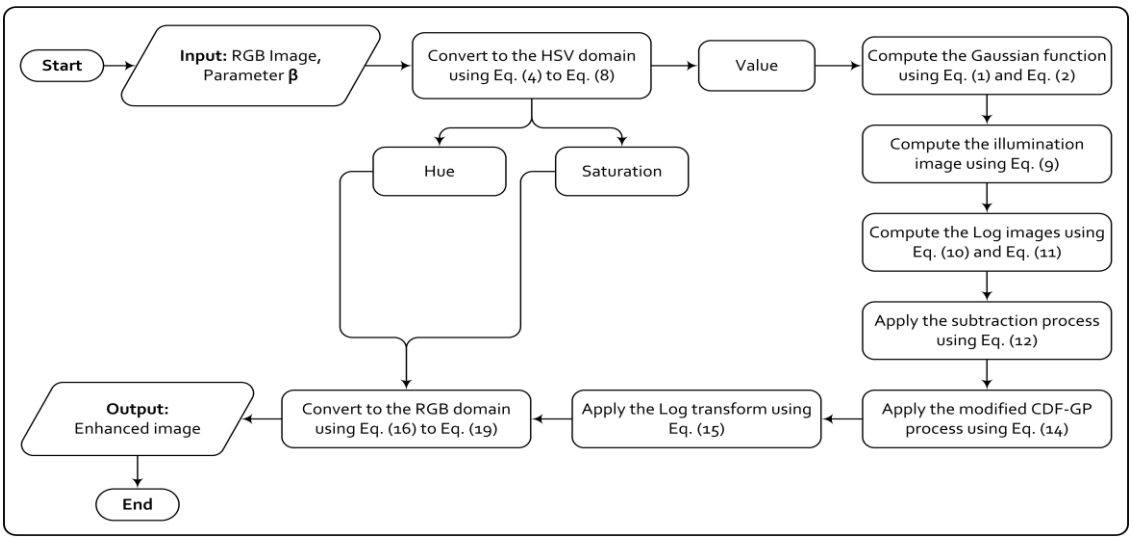

Figure 3. Flowchart of the proposed RSSR algorithm.

4. RESULTS AND DISCUSSION

In this section, the results of the proposed algorithm are presented and its performance is evaluated on low-light nighttime images. These results are also discussed and compared to the results of other algorithms. In this study, two datasets were used. The first is the MIT-Adobe FiveK dataset [24], which contains five thousand images captured using single-lens (SLR) cameras by different photographers, wherein the images are all in RAW format, meaning that all data captured by the camera sensor is pristine. Photoshop was used to convert these images from the DNG format into the JPG format. The second one is the exclusively Dark (ExDARK) dataset [25], containing approximately seven thousand images captured in low-light conditions.

When it comes to the comparison, the proposed algorithm is compared with ten advanced methods; namely, SDD [7], AIE [9], FBE [12], LECARM [10], LIME [13], RBMP [8], RRM [11], SPV [32], TS [33] and GM [34]. Moreover, the results of the proposed method and other methods are evaluated using one reduced-reference (RR) metric, called the lightness order error (LOE) and two no-reference (NR) metrics that are natural image-quality evaluator (NIQE) metric and blind/referenceless image spatial quality evaluator (BRISQUE). The LOE [27] is utilized to measure the error of the lightness order (i.e., illumination quality) between the degraded image and its filtered counterpart. The output of the LOE is a numerical value, where lower scores represent a better illumination quality. The LOE is defined as:

$$LOE = \frac{1}{W \cdot H} \cdot \sum_{x=1}^{W} \sum_{y=1}^{H} D_{(x,y)} \tag{20}$$

The variables W and H represent the image dimensions and $D_{(x,y)}$ denotes the relative order difference in luminance between two given images. Moreover, the NIQE [28] measures the naturality and evaluates the quality based on measurable deviations from statistical patterns found in natural images without considering expected distortions or human subjective judgments. The quality of the distorted image is quantified by measuring the difference between the statistical properties of the model and the distorted image. The output NIQE is a numeric value, where lower scores represent better naturality. Likewise, the BRISQUE [29] measures the distortions and perceived quality and utilizes natural scene statistics (NSS) to construct a distortion-agnostic no-reference metric for image quality that functions in the spatial domain. NSS focuses on analyzing the statistical patterns seen in “natural scene” photos and developing metrics to quantify the extent to which the statistical properties of an unfamiliar image differ from those of typical natural scene images. The output BRISQUE is a numeric value, where lower scores represent low distortion and high quality, which is deemed better. In brief, the NIQE measures the naturality, the LOE measures the illumination quality and the BRISQUE measures the existence of distortions.

As for computational complexity, CPU runtime can deliver insights into an algorithm’s efficiency and complexity [26]. Let’s dissect it: the computational complexity measures the number of resources required by a method to solve a problem. It’s usually quantified in terms of space and time complexity. The CPU runtime, on the other hand, denotes the real time needed by a CPU to implement a specific method. It relies on numerous aspects, such as the method’s complexity, the input size and the hardware utilized. Comparative analysis (CA) can be applied to this case. CA means that comparing the CPU runtimes of various methods for the same task provides a sense of relative computational complexities, in that a method with a lower runtime for the same input size denotes a lower computational complexity. Thus, CPU runtimes have been considered as a computational complexity measure and provided in this study in Table 4 and Figure 13. The computer on which experiments and evaluations were performed had specifications of 16 GB of RAM, a Core i7-8650U 2.11 GHz processor and MATLAB 2020a. Figures 4-7 show the experimental results of the proposed algorithm with various degraded nighttime images, Figures 8-11 demonstrate the comparison results. Moreover, Tables 1-4 show the recorded scores and implementation times for the compared algorithms. Finally, Figure 12 and Figure 13 display the graphs of the average performance in Tables 1-4.

As in the given samples of the conducted experiments, the proposed algorithm succeeded in improving the quality of nighttime images in that it illuminates dark areas while preserving the illumination of the bright regions from being extremely amplified, in addition to emphasizing the visual details of the filtered images. This balance benefits in maintaining the natural illumination while improving visibility in darker image parts. Moreover, the output images from the proposed RSSR algorithm have vibrant,

eye-comforting colors with acceptable contrast, bearing in mind that the proposed method does not add any distortion or unwanted artifacts during the processing procedure and prevents the noise from being massively augmented. This guarantees that the processed images stay true to the pristine scene without

Figure 4. Experimental results of the MIT-Adobe dataset **(Batch-1)**: (1st row) represents unprocessed nighttime images; (2nd row) represents the version of the enhanced images from the proposed algorithm with β values equal to (5, 6, 7, 5, 6).

Figure 5. Experimental results of the MIT-Adobe dataset **(Batch-2)**: (1st row) represents unprocessed nighttime images; (2nd row) represents the version of the enhanced images from the proposed algorithm with β values equal to (7, 6, 7, 7, 6).

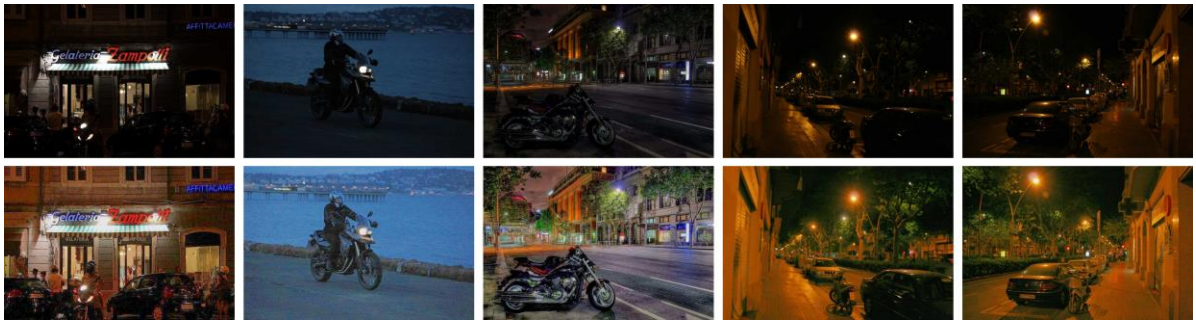

Figure 6. Experimental results of the ExDARK dataset **(Batch-1)**: (1st row) represents unprocessed nighttime images; (2nd row) represents the version of the enhanced images from the proposed algorithm with β values equal to (11, 9, 9, 10, 10).

Figure 7. Experimental results of the ExDARK dataset **(Batch-2)**: (1st row) represents unprocessed nighttime images; (2nd row) represents the version of the enhanced images from the proposed algorithm with β values equal to (12, 11, 10, 9, 9).

presenting any visual irregularities. Moreover, this also indicates that the RSSR algorithm not only enhances visibility, but also improves the images' visual appeal. In addition, the calculations are low and therefore, the proposed method has great potential in night-image processing, making it suitable for resource-constrained applications.

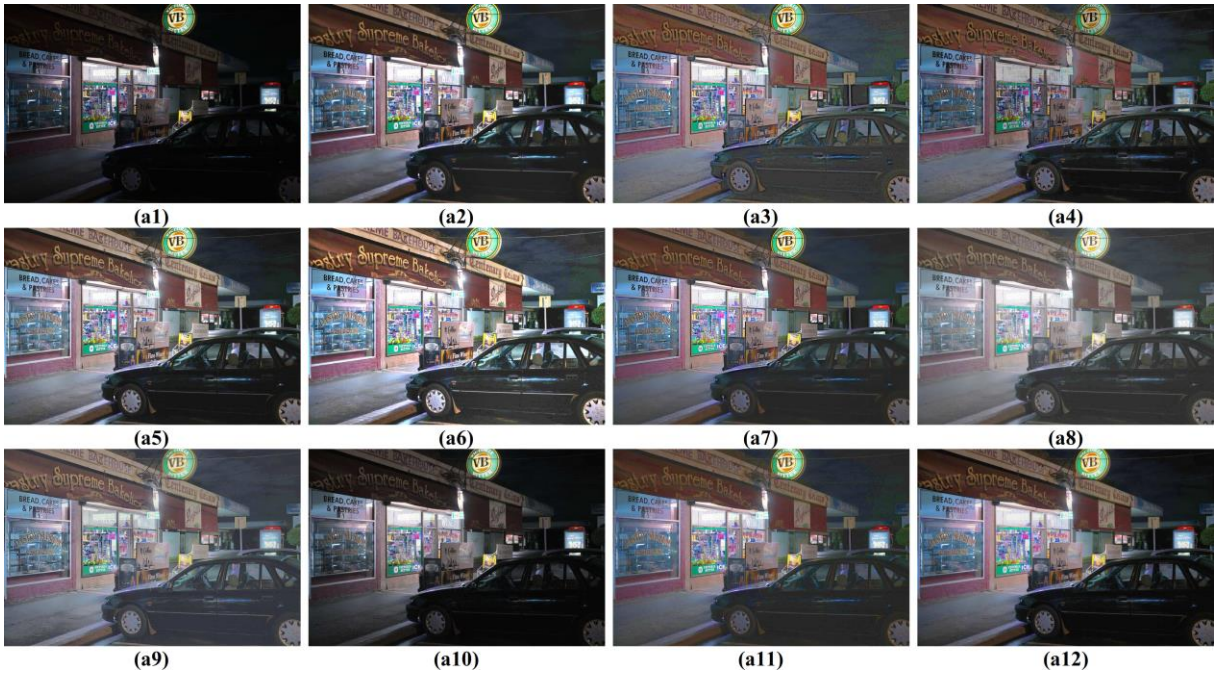

Figure 8. Comparison results **(Batch-1)**. (a1) unprocessed image (1024×683); (a2) SDD; (a3) AIE; (a4) FBE; (a5) LECARM; (a6) LIME; (a7) RRM; (a8) RBMP; (a9) GM; (a10) TS; (a11) SPV; (a12) proposed RSSR.

From the outcomes of the performed comparisons, it is observed that each method provides different enhancement modes due to the different used processing notions, wherein the analysis of each method depends on aspects, such as quality of illumination, contrast, colors, sharpness, in addition to the generation or increase in noise, artifacts or errors. SDD provided insufficient illumination with a smoothed appearance and brightness amplification. It's why the metrics readings are low and the processing speed is slow due to the implementation of the noise-reduction process. AIE delivered the second-best reading in terms of LOE compared to the other methods. However, the unnatural tonality and noise generation led to scoring poorly in NIQE and not good in BRISQUE. Still, it recorded the second fastest method in terms of processing time. FBE recorded low and unusual brightness and contrast but with adequate sharpness. Thus, LOE readings were not good, but BRISQUE and NIQE readings were agreeable and the processing speed was considered acceptable.

Likewise, LECARM produced images with insufficient lighting and had white shadows around the edges. Thus, LOE readings were unacceptable, but the BRISQUE and NIQE readings were reasonable with relatively fast processing speeds. LIME introduced brightness amplification, unusual illumination, processing errors and boosted colors. That is why the LOE readings were the worst among the competitors, yet they averaged in terms of BRISQUE and NIQE with above-average processing speed. In addition, the RRM algorithm provided average illumination with over-smoothness. Due to that, the LOE readings were mediocre, but due to the over-smoothness, the readings of BRISQUE and NIQE were very low. As for the processing time, it was the worst as it took an extremely long processing period. Moreover, RBMP delivered adequate illumination with somewhat pale colors. Thus, the LOE readings were satisfactory as well and the BRISQUE and NIQE metrics recorded the second-best results, considering that it did not generate distortions, provided slightly pale colors and was noticeable fast.

GM delivered results with limited brightness, imbalanced contrast and slightly pale colors, scoring below average in LOE, low in BRISQUE and NIQE and with slow performance according to the average runtime. TS proved to have low illumination and artifacts in the results, leading to low LOE, BRISQUE and NIQE readings with fast runtimes. SPV increased the illumination and surged the difference

between the brightest and darkest regions in the image, leading to somewhat average readings according to the utilized metrics. When it comes to the proposed RSSR, it outperformed all the other comparison algorithms subjectively and objectively, as it recorded the best readings according to LOE, BRISQUE and NIQE metrics with the fastest execution time. It is essential, because it is infrequent to have an algorithm that produces high-quality results rapidly without generating distortion or massive noise presentation. In this context, the proposed algorithm excels and its performance is considered positive and distinctive for the desired purpose, improving the illumination of nighttime images.

Figure 9. Comparison results **(Batch-2)**. (b1) unprocessed image (1024×680); (b2) SDD; (b3) AIE; (b4) FBE; (b5) LECARM; (b6) LIME; (b7) RRM; (b8) RBMP; (b9) GM; (b10) TS; (b11) SPV; (b12) proposed RSSR.

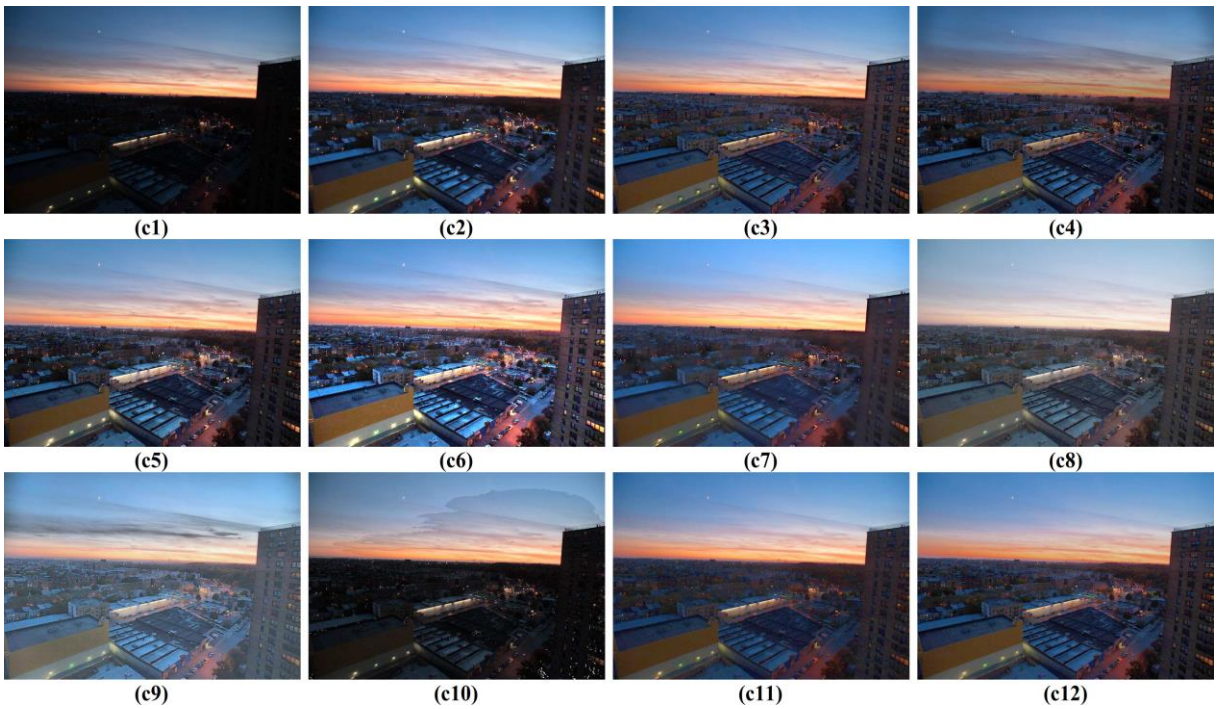

Figure 10. Comparison results **(Batch-3)**. (c1) unprocessed image (800×532); (c2) SDD; (c3) AIE; (c4) FBE; (c5) LECARM; (c6) LIME; (c7) RRM; (c8) RBMP; (c9) GM; (c10) TS; (c11) SPV; (c12) proposed RSSR.

Figure 11. Comparison results **(Batch-4)**. (d1) unprocessed image (640×427); (d2) SDD; (d3) AIE; (d4) FBE; (d5) LECARM; (d6) LIME; (d7) RRM; (d8) RBMP; (d9) GM; (d10) TS; (d11) SPV; (d12) proposed RSSR.

Table 1. The recorded LOE↓ scores.

Image	SDD	AIE	FBE	LECARM	LIME	RRM	RBMP	SPV	TS	GM	Proposed
Fig.8	310.6972	13.3393	285.7465	140.5607	619.3701	175.1018	6.8974	103.5646	100.0498	246.3067	0.9549
Fig.9	283.3439	12.1001	298.9320	172.7044	543.7599	210.1371	35.6361	167.4058	196.5971	286.8417	0.7978
Fig.10	400.8085	10.9486	376.5085	284.0700	978.8198	359.1726	34.6262	197.8955	607.2545	477.0071	7.5333
Fig.11	575.8479	11.4816	427.7972	460.4458	1087.1	571.9542	87.6679	1010.5	1589.9	395.6528	11.3453
Avg	392.6743	11.9674	347.2460	264.4452	807.2624	329.0914	41.2069	369.8414	623.4503	351.4520	**5.1578**

Table 2. The recorded BRISQUE↓ scores.

Image	SDD	AIE	FBE	LECARM	LIME	RRM	RBMP	SPV	TS	GM	Proposed
Fig.8	29.3314	34.9999	26.9860	28.0290	33.1889	31.3011	26.8401	21.8559	21.5089	28.9948	24.7420
Fig.9	28.8798	20.7151	19.1639	19.2840	20.0713	31.2884	19.7321	28.2142	17.9283	31.7083	18.0840
Fig.10	30.0810	13.0398	12.4795	12.6481	12.7708	43.1239	10.2004	23.5718	30.5554	23.8386	8.6066
Fig.11	25.2895	22.4329	18.0028	16.4182	18.8628	25.8702	17.2163	21.2278	39.0027	23.7215	15.5915
Avg	28.3954	22.7969	19.1580	19.0948	21.2234	32.8959	18.4972	23.7174	27.2488	27.0658	**16.7560**

Table 3. The recorded NIQE↓ scores.

Image	SDD	AIE	FBE	LECARM	LIME	RRM	RBMP	SPV	TS	GM	Proposed
Fig.8	2.8009	3.1575	2.3784	2.3234	2.5689	3.1398	2.3259	2.5575	2.2575	3.0323	2.1849
Fig.9	2.3427	2.9661	2.5334	2.5476	2.7440	2.8844	2.2979	2.6727	2.4478	2.7833	2.4188
Fig.10	3.3333	2.0966	2.1190	2.0112	2.1122	3.1282	2.0596	2.5849	3.1453	2.9401	1.9478
Fig.11	3.0179	3.3062	2.6004	2.7839	2.8941	3.4941	2.8951	2.9095	4.4594	3.1705	2.6001
Avg	2.8737	2.8816	2.4078	2.4165	2.5798	3.1616	2.3946	2.68115	3.0775	2.98155	**2.2879**

Table 4. The recorded runtimes↓ (in seconds).

Image	SDD	AIE	FBE	LECARM	LIME	RRM	RBMP	SPV	TS	GM	Proposed
Fig.8	21.40511	0.18263	0.84769	0.68879	2.16288	54.36626	0.45154	18.248078	0.500824	46.933321	0.13474
Fig.9	18.44903	0.18122	0.71538	0.73408	2.42125	105.09780	0.33700	22.879234	0.543656	50.913605	0.17260
Fig.10	13.30351	0.15941	0.71985	0.40115	1.10794	31.33848	0.25359	11.602561	0.310696	33.103307	0.06986
Fig.11	11.11168	0.26329	2.76838	0.37095	3.64605	36.45124	0.18027	18.511313	0.162029	16.652700	0.06114
Avg	16.06733	0.19664	1.26282	0.54874	2.33453	56.81345	0.30560	17.8102	0.37930	36.9007	**0.10958**

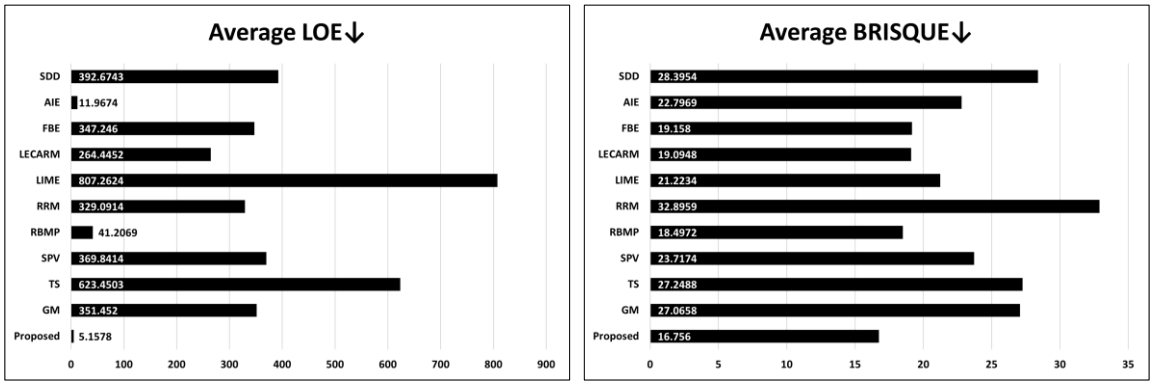

Figure 12. Average readings of LOE and BRISQUE.

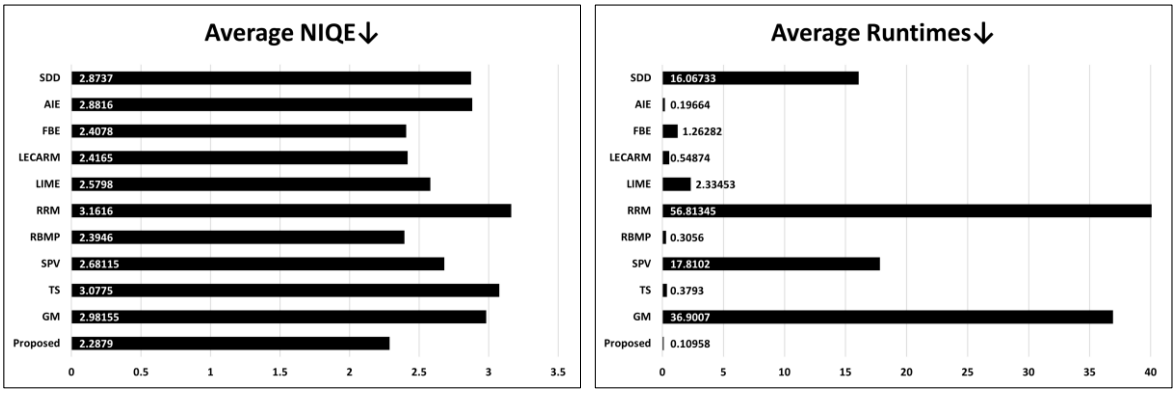

Figure 13. Average readings of NIQE and runtimes.

The proposed RSSR outperformed the other algorithms in the metrics used because of the careful development and attentive analysis of the drawbacks of the related-work methods, knowing what advantages to consider and what disadvantages to avoid. When developing the RSSR, it has been affirmed that proper illumination must be provided with balanced contrast and attractive colors and focused on avoiding the generation of unwanted processing errors in addition to evading noise amplification. Thus, the methods used in the development of the RSSR were added and adapted successfully to introduce a fast and efficient algorithm. Despite the accomplishments of the algorithm, it still has one limitation; that is, it is not fully automatic and the human operator should manually choose the value of β to produce the resulting image with the desired illumination.

5. CONCLUSION

This research proposes an algorithm to improve the illumination of nighttime images. This algorithm works on the HSV color model and estimates the illumination image in a similar way to the standard SSR model. Still, it differs in the subtraction process, as it uses logarithmic subtraction in addition to the utilization of two statistical approaches for further visual enhancement, in that the first is a modified CDF-GP approach, which applies a curvy transform and the other one is a non-complex log transform. The performance of the proposed algorithm is assessed by utilizing two different datasets. By performing a comparison with ten contemporary algorithms, the obtained results are then evaluated using three metrics and recorded CPU runtimes. The study's outcomes showed that the proposed RSSR algorithm improved the quality of nighttime images and properly illuminated the details in dark areas while avoiding over-illumination of bright areas, producing images with natural and balanced brightness, adequate colors and adjusted contrast. As a result, the proposed RSSR algorithm outperformed the other algorithms in the used objective measures and recorded the fastest runtime. This is essential, as it is challenging to find an algorithm that is uncomplicated and fast and, at the same time, generates satisfactory results. In future work, it is likely to embrace developments by including AI for automation.

ACKNOWLEDGMENT

The authors would like to thank the University of Mosul staff for the success of this study.

REFERENCES

[1] Y. F. Wang, H. M. Liu and Z. W. Fu, "Low-light Image Enhancement *via* the Absorption Light Scattering Model," IEEE Transactions on Image Processing, vol. 28, no. 11, pp. 5679–5690, 2019.

[2] X. Guo, Y. Li and H. Ling, "LIME: Low-light Image Enhancement *via* Illumination Map Estimation," IEEE Transactions on Image Processing, vol. 26, no. 2, pp. 982–993, 2017.

[3] Y. Qi et al., "A Comprehensive Overview of Image Enhancement Techniques," Archives of Computational Methods in Engineering, vol. 29, no. 1, pp. 583–607, 2022.

[4] M. Li, J. Liu, W. Yang, X. Sun and Z. Guo, "Structure-revealing Low-light Image Enhancement *via* Robust Retinex Model," IEEE Transactions on Image Processing, vol. 27, no. 6, pp. 2828–2841, 2018.

[5] H. Lee, "Successive Low-light Image Enhancement Using an Image-adaptive Mask," Symmetry (Basel), vol. 14, no. 6, p. 1165, 2022.

[6] R. R. Hussein, Y. I. Hamodi and R. A. Sabri, "Retinex Theory for Color Image Enhancement: A Systematic Review," Int. J. Electr. Comput. Eng. (IJECE), vol. 9, no. 6, p. 5560, 2019.

[7] S. Hao, X. Han, Y. Guo, X. Xu and M. Wang, "Low-light Image Enhancement with Semi-decoupled Decomposition," IEEE Transactions on Multimedia, vol. 22, no. 12, pp. 3025–3038, 2020.

[8] M. A. Al-Hashim and Z. Al-Ameen, "Retinex-based Multiphase Algorithm for Low-light Image Enhancement," Traitement du Signal (TS), vol. 37, no. 5, pp. 733–743, 2020.

[9] W. Wang, Z. Chen, X. Yuan and X. Wu, "Adaptive Image Enhancement Method for Correcting Low-illumination Images," Information Sciences, vol. 496, pp. 25–41, 2019.

[10] Y. Ren, Z. Ying, T. H. Li and G. Li, "LECARM: Low-light Image Enhancement Using the Camera Response Model," IEEE Trans. on Circuits and Sys. for Video Techn., vol. 29, no. 4, pp. 968–981, 2019.

[11] M. Li, J. Liu, W. Yang, X. Sun and Z. Guo, "Structure-revealing Low-light Image Enhancement *via* Robust Retinex Model," IEEE Transactions on Image Processing, vol. 27, no. 6, pp. 2828–2841, 2018.

[12] X. Fu, D. Zeng, Y. Huang, Y. Liao, X. Ding and J. Paisley, "A Fusion-based Enhancing Method for Weakly Illuminated Images," Signal Processing, vol. 129, pp. 82–96, 2016.

[13] X. Guo, "LIME: A Method for Low-light Image Enhancement," Proc. of the 24th ACM Int. Conf. on Multimedia, DOI:10.1145/2964284.2967188, 2016.

[14] D. J. Jobson, Z. Rahman and G. A. Woodell, "Properties and Performance of a Center/Surround Retinex," IEEE Transactions on Image Processing, vol. 6, no. 3, pp. 451-462, 1997.

[15] Z. Rahman, D. J. Jobson, and G. A. Woodell, “Resiliency of the multiscale retinex image enhancement algorithm,” in Color Imaging Conference: Color Science, Systems and Applications, 1998.

[16] D. J. Jobson, "Retinex Processing for Automatic Image Enhancement," Journal of Electronic Imaging, vol. 13, no. 1, pp. 100-110, 2004.

[17] M. Ismail and Z. Al-Ameen, "Adapted Single Scale Retinex Algorithm for Nighttime Image Enhancement," AL-Rafidain J. of Computer Sciences and Mathematics, vol. 16, no. 1, pp. 59–69, 2022.

[18] Y. Meng, D. Kong, Z. Zhu and Y. Zhao, "From Night to Day: GANs Based Low Quality Image Enhancement," Neural Processing Letters, vol. 50, no. 1, pp. 799–814, 2019.

[19] R. C. Gonzalez and R. E. Woods, Digital Image Processing: International Edition, 3rd Ed., Upper Saddle River, NJ: Pearson, 2008.

[20] V. Patrascu and V. Buzuloiu, "Color Image Processing Using Logarithmic Operations," Proc. of the IEEE Int. Symposium on Signals, Circuits and Systems (SCS 2003), DOI: 10.1109/SCS.2003.1226966, 2004.

[21] R. J. Oosterbaan, "Software for Generalized and Composite Probability Distributions," International Journal of Mathematical and Computational Methods, vol. 4, no. 1, pp. 1-19, 2019.

[22] W. Wang, X. Wu, X. Yuan and Z. Gao, "An Experiment-based Review of Low-light Image Enhancement Methods," IEEE Access, vol. 8, pp. 87884–87917, 2020.

[23] E. Baidoo and K. Alex, "Implementation of Gray Level Image Transformation Techniques," Int. J. of Modern Education and Computer Science, vol. 10, no. 5, pp. 44–53, 2018.

[24] V. Bychkovsky, S. Paris, E. Chan and F. Durand, "Learning Photographic Global Tonal Adjustment with a Database of Input/Output Image Pairs," Proc. of the Int. Conf. on Computer Vision and Pattern Recognition (CVPR), DOI: 10.1109/CVPR.2011.5995413, Colorado Springs, USA, 2011.

[25] Y. P. Loh and C. S. Chan, "Getting to Know Low-light Images with the Exclusively Dark Dataset," Computer Vision and Image Understanding, vol. 178, pp. 30–42, 2019.

[26] M. R. Lone and A. K. Sandhu, "Enhancing Image Quality: A Nearest Neighbor Median Filter Approach for Impulse Noise Reduction," Multimedia Tools and Applications, pp. 1–17, 2023.

[27] S. Bao, S. Ma and C. Yang, “Multi-scale retinex-based contrast enhancement method for preserving the naturalness of color image,” Opt. Rev., vol. 27, no. 6, pp. 475–485, 2020.

[28] A. Mittal, R. Soundararajan and A. C. Bovik, "Making a ‘Completely Blind’ Image Quality Analyzer," IEEE Signal Processing Letters, vol. 20, no. 3, pp. 209–212, 2013.

[29] A. Mittal, A. K. Moorthy and A. C. Bovik, "No-reference Image Quality Assessment in the Spatial Domain," IEEE Transactions on Image Processing, vol. 21, no. 12, pp. 4695–4708, 2012.

[30] E. H. Land and J. J. McCann, "Lightness and Retinex Theory," J. of the Optical Society of America, vol.

61, no. 1, pp. 1–11, 1971.
[31] W. Burger and M. Burge, Principles of Digital Image Processing: Fundamental Techniques, 1st Edn. London, England: Springer, 2009.
[32] X. Wu, B. Wu, J. He, B. Fang, Z. Shang and M. Zhou, "A Structure Preservation and Denoising Low-light Enhancement Model *via* Coefficient of Variation," Int. J. of Pattern Recognition and Artificial Intelligence, vol. 36, no. 13, DOI: 10.1142/S0218001422540180, 2022.
[33] M. F. Hassan, T. Adam, H. Rajagopal and R. Paramesran, "A Hue Preserving Uniform Illumination Image Enhancement *via* Triangle Similarity Criterion in HSI Color Space," Visual Computer, vol. 39, no. 12, pp. 6755–6766, 2023.
[34] X. Yi, C. Min, M. Shao, H. Zheng and Q. Lv, "Low-light Image Enhancement *via* Regularized Gaussian Fields Model," Neural Processing Letters, vol. 55, no. 9, pp. 12017–12037, 2023.
[35] J. J. Jeon, J. Y. Park and I. K. Eom, "Low-light Image Enhancement Using Gamma Correction Prior in Mixed Color Spaces," Pattern Recognition, vol. 146, p. 110001, DOI: 10.1016/j.patcog.2023.110001, 2024.
[36] J. Li, X. Feng and Z. Hua, "Low-light Image Enhancement *via* Progressive-recursive Network," IEEE Transactions on Circuits and Systems for Video Technology, vol. 31, no. 11, pp. 4227–4240, 2021.
[37] D. Dai and L. Van Gool, "Dark Model Adaptation: Semantic Image Segmentation from Daytime to Nighttime," Proc. of the 21st Int. Conf. on Intelligent Transportation Systems (ITSC), DOI: 10.1109/ITSC.2018.8569387, Maui, USA, 2018.

ملخص البحث:

في هذه الأيام، يُمارِس النّاس نشاطاتٍ في اللّيلِ ويلتقطون العديدَ من الصّور لتوثيق نشاطاتهم. ونظراً لضعْف الإضاءة في البيئة اللّيلية، تميل الصّور الملتقطة ليلاً إلى الظُّهور بإضاءةٍ مُعتِمة وغير متوازنة، وتباينٍ محدود، وضجيجٍ كبير، وألوانٍ غير واضحةٍ.

تقترح هذه الورقة خوارزميةً عمليةً لتحسين الإضاءة في الصُّور اللّيلية باستخدام نموذجٍ يرتكز على طُرقٍ لمعالجة الصّور وعددٍ من الدّوالّ الاحصائية. يبدأ النّموذج المستَخدم بتحويل الصّور المراد معالجتها من نموذج (أحمر أخضر أزرق RGB) إلى نموذج (HSV)، ثم يحسّن فقط قناة (V) مُبقياً على قناة (H) وقناة (S). بعد ذلك، يتمّ تقدير نسخة الإضاءة من الصّورة وحساب خوارزميات كلٍّ من الإضاءة والصّورة الأصلية.

بعدئذٍ، تحدث عملية طرح لوغاريثمي، ويتمّ تطبيق دّالة توزيع تراكمية للإحتمالية، وتكون النتيجة مزيداً من التّحسين باستخدام طريقة نقل لوغاريثمية. وتؤدي هذه العمليات إلى إنتاج قناة (V) المعالجة إلى جانب التّحويل إلى نموذج (RGB) للحصول على المخرج النّهائي.

لقد تمّ تجريبُ النّموذج المقترح باستخدام مجموعتي بياناتٍ، ومقارنته مع عشر خوارزميات واردة في أدبيات الموضوع باستخدام ثلاثةٍ من مؤشرات القياس. وبناءً على نتائج المقارنة، تمّ الحصول على مؤشّرات أداءٍ واعدةٍ للنّموذج المقترح تفوق مؤشرات الأداء في كثيرٍ من الخوارزميات القائمة التي تهدف إلى تحسين الإضاءة في الصّور الملتقطة ليلاً.